Table 2 Validated somatic non-synonymous substitutions and small indels in coding regions of a liver cancer genome

Gene	Chr.	Strand	Position	Allele change	Amino acid change	Copy number	Mutant allele (%) in whole-genome sequencing	Mutant allele (%) in whole-exome sequencing	Expression ratio (T/N)	Functional
PLEKHG5	1	–	6,452,224	G>T	Asp>Tyr	N	49.0	27.7	1.86	Deleterious
KIAA1026	1	+	15,294,007	C>A	Ala>Glu	N	45.7	nd	0.15	Tolerated
MYCL1	1	–	40,139,080	T>G	Phe>Cys	N	54.5	nd	1.93	Tolerated
PDE4B	1	+	66,231,185	C>A	Ala>Glu	N	57.1	42.9	0.83	Tolerated
CLCC1	1	–	109,284,236	A>G	Tyr>Cys	N	33.3	39.3	1.61	Deleterious
CNRIP1	2	–	68,397,833	C>T	Thr>Met	N	40.0	33.3	1.39	Deleterious
ANKRD36	2	+	97,181,397	A>G	Lys>Glu	N	17.8	nd	9.49	Tolerated
UBR3	2	+	170,511,073	A>C	Glu>Asp	N	57.1	nd	18.10	Tolerated
CUL3	2	–	225,070,790	G>A	Ser>Asn	N	42.9	52.8	12.80	Tolerated
COPS7B	2	+	232,369,129	A>G	Ile>Val	N	44.4	41.5	1.82	Tolerated
RAF1	3	–	12,625,811	A>G	Asn>Ser	N	40.0	50.0	2.31	Tolerated
ITIH3	3	+	52,813,002	A>G	Met>Val	N	43.9	nd	1.25	Deleterious
ERC2	3	–	56,148,636	G>C	Glu>Gln	N	40.0	nd	1.33	Tolerated
TBC1D23	3	+	101,496,868	del AAG	Deletion (E)	N	14.8	nd	4.90	na
ATR	3	–	143,671,657	del AT	Deletion (frame shift)	N	20.0	nd	4.49	na
SLC7A14	3	–	171,701,666	G>A	Ser>Asn	N	52.8	46.3	2.19	Deleterious
PCDH7	4	+	30,333,134	G>A	Arg>His	N	47.1	47.8	1.74	Tolerated
FAM13A	4	–	89,872,188	A>T	His>Leu	N	52.0	47.4	0.85	Tolerated
MFSD8	4	–	129,090,435	A>T	Met>Leu	Loss	62.5	74.3	1.15	Tolerated
DMGDH	5	–	78,375,996	T>A	Leu>Gln	N	50.0	37.6	3.04	Tolerated
PCDHA13	5	+	140,244,063	C>T	Pro>Ser	N	45.1	34.8	na	Deleterious
CCDC99	5	+	168,960,950	T>G	Ser>Arg	N	37.1	39.4	13.30	Deleterious
GABBR1	6	–	29,706,345	C>T	Thr>Met	N	42.0	37.8	0.59	Tolerated
CSNK2B	6	+	31,745,659	A>T	Ser>Cys	N	37.3	nd	1.41	Deleterious
MOCS1	6	–	40,003,210	G>T	Ser>Ile	N	34.4	nd	1.54	Tolerated
GTPBP2	6	–	43,699,685	A>T	Glu>Val	N	58.0	56.3	1.36	Tolerated
KHDRBS2	6	–	62,662,692	G>T	Arg>Leu	N	34.1	nd	0.88	Deleterious
SLC29A4	7	+	5,303,324	A>T	His>Leu	N	43.8	nd	7.00	Deleterious
TMEM195	7	–	15,567,887	C>G	Pro>Ala	N	41.2	38.3	1.03	Deleterious
RFC2	7	–	73,302,032	A>T	Glu>Asp	N	26.0	41.9	1.09	Tolerated
ADAM22	7	+	87,653,951	A>T	Arg>Trp	N	41.2	39.1	0.55	Deleterious
TRRAP	7	+	98,417,359	G>T	Trp>Leu	N	39.0	nd	2.07	Deleterious
XRCC2	7	–	151,977,231	G>A	Arg>Gln	N	56.2	36.5	4.18	Deleterious
MTDH	8	+	98,781,211	G>T	Val>Phe	N	33.3	46.9	14.40	Tolerated
SLA	8	–	134,141,539	C>A	Pro>Thr	N	43.6	nd	1.18	Deleterious
JAK2	9	+	5,045,703	T>G	Ile>Ser	Loss	100.0	84.2	4.84	Tolerated
NTRK2	9	+	86,532,391	G>A	Ala>Thr	Loss	90.0	85.9	0.84	Tolerated
TSC1	9	–	134,767,848	C>T	Arg>stop	Loss	13.3	13.0	1.85	Deleterious
CREM	10	+	35,496,706	A>G	Glu>Gly	N	44.8	42.3	3.28	Tolerated
C10orf95	10	–	104,200,839	T>C	Cys>Arg	N	39.7	nd	3.05	Tolerated
PSTK	10	+	124,730,061	C>T	Leu>Phe	N	53.6	nd	6.94	Deleterious
ATHL1	11	+	283,903	C>T	Ala>Val	N	40.9	26.8	1.12	Tolerated
MUC5B	11	+	1,213,214	G>T	Val>Leu	N	33.8	nd	0.83	Tolerated
DENND5A	11	–	9,181,879	C>T	Pro>Ser	N	21.4	29.9	2.43	Deleterious
GIF	11	–	59,369,438	C>T	Thr>Ile	AMP (3)	29.2	nd	0.83	Tolerated
STIP1	11	+	63,719,763	G>A	Glu>Lys	Loss	66.7	nd	1.28	Tolerated
FAT3	11	+	91,727,805	C>G	Thr>Ser	Loss	73.1	nd	na	Tolerated
PTMS	12	+	6,749,421	A>G	Glu>Gly	Loss	55.0	nd	0.56	Tolerated
ARID2	12	+	44,530,716	ins T	Insertion (frame shift)	N	31.9	nd	2.35	na
C12orf51	12	–	111,134,825	del CCTGCCACGTCA	Deletion (GDVA)	N	21.6	nd	1.44	Torelated
RBM19	12	–	112,868,641	C>T	Pro>Leu	N	49.3	42.2	1.32	Deleterious
AACS	12	+	124,142,015	G>T	Gly>Val	N	34.9	26.0	1.75	Deleterious
KHNYN	14	+	23,971,333	del CCT	Deletion (L)	N	24.1	nd	2.17	Tolerated
NOVA1	14	–	25,987,233	A>T	Leu>Phe	N	36.7	38.1	0.91	Tolerated
LTBP2	14	–	74,045,780	G>A	Gly>Glu	N	38.1	nd	3.43	Deleterious
CYFIP1	15	+	20,498,517	C>T	Ala>Val	N	55.1	41.4	1.88	Deleterious
GABRB3	15	–	24,357,328	G>T	Met>Ile	N	39.4	43.4	0.15	Tolerated
EID1	15	+	46,957,688	C>G	Ser>Cys	N	40.4	nd	8.60	Deleterious
HCN4	15	–	71,402,254	G>A	Arg>His	N	43.6	nd	0.61	Tolerated
AKAP13	15	+	84,060,152	del T	Deletion (frame shift)	N	34.5	nd	0.88	na
AXIN1	16	–	287,910	C>T	Arg>stop	Loss	78.7	nd	0.94	Deleterious
LITAF	16	–	11,554,943	del G	Deletion (frame shift)	Loss	61.3	nd	0.97	na
TP53	17	–	7,518,985	G>T	Val>Leu	Loss	78.0	73.1	0.06	Deleterious
NEK8	17	+	24,092,271	G>A	Gly>Asp	N	36.7	39.1	1.44	Deleterious
CPD	17	+	25,773,820	A>G	Tyr>Cys	N	47.1	52.3	2.28	Deleterious
LRRC30	18	+	7,221,594	C>G	Ser>Cys	N	52.0	45.6	na	Deleterious
ZNF560	19	–	9,439,794	A>C	Ile>Leu	N	58.8	48.3	0.86	Tolerated
SCRT2	20	–	593,073	T>A	Tyr>Asn	N	53.7	nd	0.51	Deleterious
USP25	21	+	16,119,227	C>T	Thr>Met	N	44.4	nd	13.00	Deleterious
USP25	21	+	16,125,626	A>C	Glu>Asp	N	35.3	38.1	na	Tolerated
ARVCF	22	–	18,341,717	C>G	Ser>Cys	N	53.0	50.0	1.30	Deleterious
USP26	X	–	131,988,824	T>C	Leu>Pro	AMP (4)	93.8	94.4	0.85	Tolerated

Except for *ANKRD36* and *TSC1*, all 63 somatic non-synonymous substitutions were predicted by whole-genome sequencing and in-house informatics method using stringent analysis criteria (Online Methods). One somatic missense substitution in *ANKRD36* was predicted under less stringent criteria. One somatic nonsense substitution in *TSC1* was predicted only by whole-exome sequencing. Chr., chromosome; N, copy neutral; AMP, amplicon; nd, not detected; na, not applicable.

Table 3 Validated somatic structural alterations in a liver cancer genome

Type	Chr. A	Break point A	CNV (Chr. A)	Chr. B	Break point B	CNV (Chr. B)	Intervening sequence	Associated genes	Fusion genes
Deletion	3	111,866,468	BCNC	3	111,868,894	BCNC	0		
Deletion	4	57,529,004	BCNC	4	57,530,452	BCNC	0	*C4orf14* (exon 4 is deleted)	
Deletion	4	92,895,135	BCNC	4	93,151,201	BCNC	0		
Deletion	5	18,130,563	BCNC	5	18,133,946	BCNC	(+) 29bp		
Deletion	6	90,130,109	BCNC	6	90,819,100	BCNC	0	*LYRM2, ANKRD6, BACH2, MDN1, CASP8AP2, RRAGD, GJA10*	
Deletion	7	69,321,043	N	7	69,404,639	N	0	*AUTS2*	
Deletion	9	132,763,157	BCNC	9	132,764,920	BCNC	0		
Deletion	10	75,477,784	BCNC	10	75,956,310	BCNC	(+) 1 bp	*AP3M1, VCL, ADK*	*VCL, ADK*
Deletion	11	67,126,436	BCNC	11	68,254,241	BCNC	0	*SUV420H1, SAPS3, ACY3, ALDH3B2, CHKA, TCIRG1, LRP5, GAL, ALDH3B1, TBX10, NDUFV1, UNC93B1, NUDT8, C11orf24*	
Deletion	15	47,394,203	BCNC	15	47,467,920	BCNC	0	*GALK2, C15orf33*	
Deletion	17	15,902,440	BCNC	17	16,056,159	BCNC	0	*NCOR1* (homozygous deletion)	
Inversion	4	60,946,299	N	4	60,947,151	N	0		
Inversion	4	172,703,199	Loss	4	172,706,239	Loss	(+) 4bp		
Inversion	11	57,305,269	BCNC	11	62,352,275	BCNC	0	*CTNND1* (UTR), *STX5*	*CTNND1, STX5*
Inversion	11	57,770,822	BCNC	11	67,133,985	BCNC	0	*NDUFV1*	
Inversion	11	62,309,952	BCNC	11	70,746,006	BCNC	0	*TAF6L*	
Inversion	11	69,067,231	AMP	11	69,317,424	AMP	0		
Inversion	11	69,093,978	AMP	11	69,098,117	AMP	0		
Inversion	11	69,871,206	AMP	11	69,877,391	AMP	(+) 6bp	*PPFIA1*	
Inversion	X	129,015,072	N	X	129,029,501	BCNC	(+) 23bp	*BCORL1, ELF4*	*BCORL1, ELF4*
Inversion	X	129,016,981	N	X	129,031,425	BCNC	0	*BCORL1, ELF4*	*BCORL1, ELF4*
Tandem duplication	11	67,043,308	BCNC	11	67,318,685	BCNC	0	*ACY3, ALDH3B2, GSTP1, TBX10, NDUFV1, NUDT8, CABP2, LOC645332*	*CABP2, LOC645332*
Translocation	11	69,316,960	AMP	X	129,030,346	BCNC	0	*ELF4*	

The inversions at Xq25 occurred from one rearrangement event and the total number of inversion is counted as nine. Chr., chromosome; BCNC, boundary of copy number change; N, copy neutral; AMP, amplicon.

which harbors only the rearranged allele (**Fig. 2d** and **Supplementary Fig. 9**). We screened for the presence of these four chimera transcripts by RT-PCR, but we detected no recurrent fusion event in 47 cases of primary HCC, possibly due to the low frequency of these rearrangements in HCC or because of the technical difficulty in detecting all variant fusion transcripts.

We also sequenced the whole exomes of the same samples using an in-solution gene enrichment system[5] (**Fig. 3a**). Capture probes for whole-exome sequencing were designed to cover the protein coding exons using the consensus coding sequences, excluding highly homologous regions. The average coverage of the whole exome sequences (41.3 Mb in total) was about twice (76.8× for HCC and 74.3× for lymphocytes) that of the whole genome sequences and had one twelfth of the total sequence amount (8.9 Gb for HCC and 8.6 Gb for lymphocyte) (**Supplementary Table 3**). Whole-exome sequencing detected 47 non-synonymous somatic substitutions, 40 of which were validated by Sanger sequencing. Among the validated substitutions, a nonsense substitution (p.Arg785X) in *TSC1*, located in the hemizygous region (9q34), was not detected by whole-genome sequencing (**Fig. 3b**). Capillary sequencing validated the same substitution with a very low

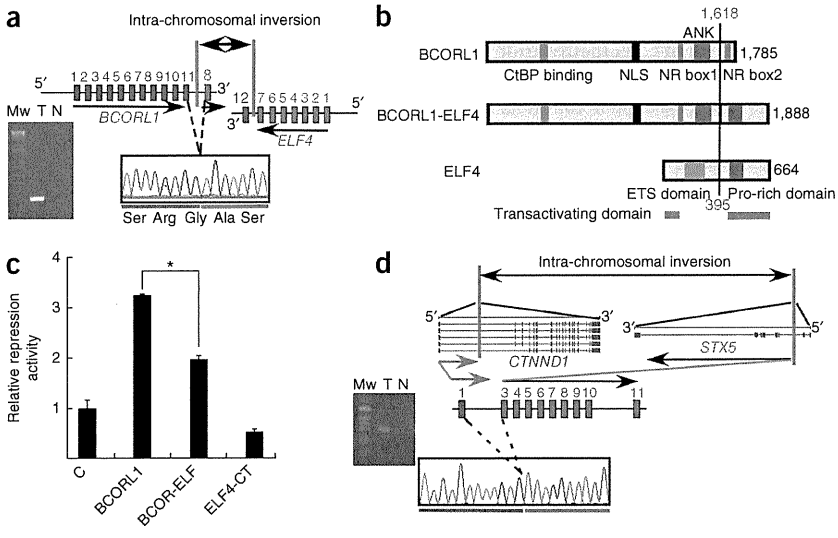

Figure 2 Characterization of rearrangements in liver cancer. (**a**) Top, schematic representation of the intra-chromosomal inversion at Xq25. Bottom left, RT-PCR analysis of the fused *BCORL1-ELF4* transcript in tumor (T) and non-cancerous liver (N) tissues. We detected no *ELF4-BCORL1* transcript (data not shown). Bottom right, sequence chromatography of the fusion transcript revealed an in-frame protein. Mw, molecular marker. (**b**) Schematic representation of the BCORL1-ELF4 fusion protein. BCORL1 (top) contains a CtBP1 binding domain (PXDLS sequence), a binuclear localization signal (NLS), two LXXLL nuclear receptor recruitment motifs (NR box) and tandem ankyrin repeats (ANK). ELF4 (bottom) contains an ETS (E Twenty Six) DNA binding domain and a proline-rich domain. Transactivating domains are indicated by the red bars[16]. The BCORL1-ELF4 chimeric protein includes most of BCORL1 (1–1,618 amino acids) lacking the NR box2 and the carboxyl-terminal portion of ELF4 containing the proline-rich domain. The number of amino acids is indicated on the right. (**c**) Wild-type BCORL1, ELF4-CT (395–664 amino acids) and the BCORL1-ELF4 chimera were expressed as Gal4-DBD fusion proteins, and their relative transcriptional activities were compared to the Gal4-DBD protein (C) as shown. (**d**) Characterization of the *CTNND1-STX5* fusion gene. Bottom left, RTPCR analysis of the fused *CTNND1-STX5* transcript in tumor (T) and non-cancerous liver tissue (N). Bottom right, sequence chromatography of the fusion transcript. Data is the mean ± s.d. ($n = 3$). *$P < 0.001$.

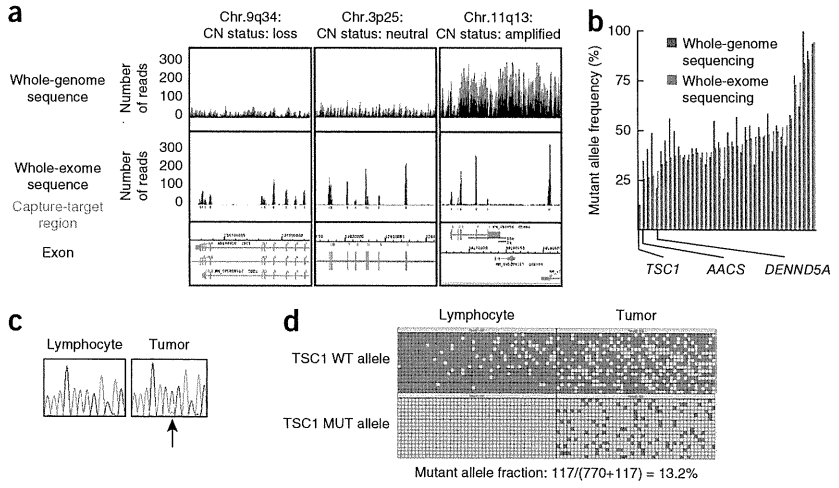

Figure 3 Intra-tumoral genetic heterogeneity detected by exon-capture sequencing. (**a**) Specific enrichment and high sequence coverage of the target genome regions indicated by the sequence viewer (copy number (CN) status is shown above). The distribution and number of reads (black, forward read; gray, reverse read) from whole-genome sequencing (top) and whole-exome sequencing (middle) are shown. The location of the capture target regions (red box) and the exons (green box) along the genome are shown at the bottom. Note that the number of reads is dependent on copy number status. (**b**) Mutant allele frequency detected by whole-genome sequencing and whole-exome sequencing. *TSC1*, *AACS* (whose heterogeneity is shown in **Supplementary Fig. 10**) and *DENND5A* are indicated. (**c**) *TSC1* mutation in the liver cancer subpopulation. Sequence chromatograms of *TSC1* in lymphocytes and whole-tumor tissue are shown. Note the small peak for the mutant T allele (indicated by the arrow) in the tumor DNA. (**d**) Determination of mutant *TSC1* allele frequency by digital PCR genotyping. WT, wild type; MUT, mutant.

signal peak (**Fig. 3c**), and digital genotyping showed that 13.2% of the tumor alleles harbored this substitution (**Fig. 3d**), suggesting that this substitution occurred in a minor population of cancer cells. Whole-exome sequencing missed 25 non-synonymous somatic substitutions that were detected by whole-genome sequencing. These missed substitutions were located in regions where sequence coverage was low or where further optimization of the probe design was required.

The number of non-synonymous somatic substitutions validated in this HCC (63) was greater than those for acute myeloid leukemia[11] (10), basal-like breast cancer[12] (22), lobular carcinoma[13] (32), glioblastoma multiforme[14] (32) and pancreatic cancer[15] (43) but is in the range of those previously reported for colorectal[16] (70) and breast[16] (88) cancer. We have shown that the pattern of somatic substitutions in a HCV-associated HCC genome is different (predominance of T>C, especially at ApT sites, and C>T, especially at CpG sites) compared to smoking-related[17,18] and ultraviolet light–related[6] cancers. Preferential C>T/G>A transition may partly be due to the higher frequency of CpG methylation in the genome sequence and is a common form of mutation in cancers[19]. Therefore, the T>C/A>G transition could be a characteristic mutational signature of HCV-associated cancer, which would be consistent with a previous observation that HCV induces error-prone DNA polymerases that preferentially cause the T>C/A>G mutation[20]. It is also possible that this mutation pattern is independent of viral infection and is organ specific, as a comparable substitution spectrum has been reported in renal cancer[19]. Additionally, only T>C changes, but not C>T changes, were effectively repaired on the transcribed strand. Similar enhanced transcription-coupled repair on preferentially acquired substitutions has been reported in other cancers[6,17,18] and could be a common phenomenon in cancer mutation.

Because single-molecule sequencing has the capability to detect every individual somatic event in parallel, higher sequence coverage will enable us to clarify the intra-tumoral heterogeneity that is associated with diverse aspects of clinical behavior such as metastasis[21]. The *TSC1* complex, which is inactivated in a subpopulation of tumors, negatively regulates the mammalian target of rapamycin signaling, which is an important oncogenic pathway related to the growth, metabolism and stemness of cancer cells[22,23], and could be a promising molecular therapeutic target in HCC progression[24].

URLs. International Cancer Genome Consortium, http://www.icgc.org/; Catalogue of Somatic Mutations in Cancer, http://www.sanger.ac.uk/genetics/CGP/cosmic/; BLASTN, ftp://ftp.ncbi.nlm.nih.gov/blast/executables/release/LATEST.

METHODS

Methods and any associated references are available in the online version of the paper at http://www.nature.com/naturegenetics/.

Note: Supplementary information is available on the Nature Genetics website.

ACKNOWLEDGMENTS

We thank K.K. Khanna (The Queensland Institute of Medical Research) for providing a human *BCORL1* cDNA clone; T.D. Taylor (RIKEN) for comments on the manuscript; T. Urushidate, S. Ohashi, S. Ohnami, A. Kokubu, N. Okada, K. Shiina, H. Meguro and K. Nakano for their excellent technical assistance. This work was supported by the Program for Promotion of Fundamental Studies in Health Sciences of the National Institute of Biomedical Innovation (NIBIO), Japan, and the Industrial Technology Research Grant Program from the New Energy and Industrial Technology Development Organization (NEDO), Japan. This study is associated with the International Cancer Genome Consortium (ICGC), and the mutation data were deposited at and released from the ICGC web site.

AUTHOR CONTRIBUTIONS

The study was designed by T. Shibata, H.A., T.Y. and J.K. Sequencing and data analyses were conducted by Y.T., K.T., S.Y., S.T., K. Sonoda and H.T. Allele typing and copy number analyses were performed by H.S. and S.I. Other molecular studies were done by Y.A., F.H., T. Shirakihara, and L.W.; H.O., K. Shimada, T.K., T.O. and K.K. coordinated collection of clinical sample and information. The manuscript was written by Y.T., T. Shibata, K.T., S.Y., H.A. and T.Y.

COMPETING FINANCIAL INTERESTS

The authors declare no competing financial interests.

Published online at http://www.nature.com/naturegenetics /.
Reprints and permissions information is available online at http://npg.nature.com/reprintsandpermissions/ .

1. El-Serag, H.B. & Rudolph, K.L. Hepatocellular carcinoma: epidemiology and molecular carcinogenesis. *Gastroenterology* **132**, 2557–2576 (2007).
2. Bentley, D.R. *et al.* Accurate whole human genome sequencing using reversible terminator chemistry. *Nature* **456**, 53–59 (2008).
3. Huang, W., Sherman, B.T. & Lempicki, R.A. Systematic and integrative analysis of large gene lists using DAVID Bioinformatics Resources. *Nat. Protoc.* **4**, 44–57 (2009).
4. Ng, S.B. *et al.* Targeted capture and massively parallel sequencing of 12 human exomes. *Nature* **461**, 272–276 (2009).

5. Gnirke, A. *et al.* Solution hybrid selection with ultra-long oligonucleotides for massively parallel targeted sequencing. *Nat. Biotechnol.* **27**, 182–189 (2009).
6. Pleasance, E.D. *et al.* A comprehensive catalogue of somatic mutations from a human cancer genome. *Nature* **463**, 191–196 (2010).
7. Xiang, Z. *et al.* Identification of somatic *JAK1* mutations in patients with acute myeloid leukemia. *Blood* **111**, 4809–4812 (2008).
8. Pagan, J.K. *et al.* A novel corepressor, BCoR-L1, represses transcription through an interaction with CtBP. *J. Biol. Chem.* **282**, 15248–15257 (2002).
9. Miyazaki, Y., Sun, X., Uchida, H., Zhang, J. & Nimer, S. MEF, a novel transcription factor with an Elf-1 like DNA binding domain but distinct transcriptional activating properties. *Oncogene* **13**, 1721–1729 (1996).
10. Suico, M.A. *et al.* Functional dissection of the ETS transcription factor MEF. *Biochim. Biophys. Acta* **1577**, 113–120 (2002).
11. Mardis, E.R. *et al.* Recurring mutations found by sequencing an acute myeloid leukemia genome. *N. Engl. J. Med.* **361**, 1058–1066 (2009).
12. Ding, L. *et al.* Genome remodelling in a basal-like breast cancer metastasis and xenograft. *Nature* **464**, 999–1005 (2010).
13. Shah, S.P. *et al.* Mutation evolution in a lobular breast tumour profiled at single nucleotide resolution. *Nature* **461**, 809–813 (2009).
14. Parsons, D.W. *et al.* An integrated genomic analysis of human glioblastoma multiforme. *Science* **321**, 1807–1812 (2008).
15. Jones, S. *et al.* Core signaling pathways in human pancreatic cancers revealed by global genomic analyses. *Science* **321**, 1801–1806 (2008).
16. Wood, L.D. *et al.* The genomic landscapes of human breast and colorectal cancers. *Science* **318**, 1108–1113 (2007).
17. Pleasance, E.D. *et al.* A small-cell lung cancer genome with complex signatures of tobacco exposure. *Nature* **463**, 184–190 (2010).
18. Lee, W. *et al.* The mutation spectrum revealed by paired genome sequences from a lung cancer patient. *Nature* **465**, 473–477 (2010).
19. Greenman, C. *et al.* Patterns of somatic mutation in human cancer genomes. *Nature* **446**, 153–158 (2007).
20. Machida, K. *et al.* Hepatitis C virus induces a mutator phenotype: enhanced mutations of immunoglobulin and protooncogenes. *Proc. Natl. Acad. Sci. USA* **101**, 4262–4267 (2004).
21. Kim, M.Y. *et al.* Tumor self-seeding by circulating cancer cells. *Cell* **139**, 1315–1326 (2009).
22. Guertin, D.A. & Sabatini, D.M. Defining the role of mTOR in cancer. *Cancer Cell* **12**, 9–22 (2007).
23. Yilmaz, O.H. *et al.* Pten dependence distinguishes haematopoietic stem cells from leukaemia-initiating cells. *Nature* **441**, 475–482 (2006).
24. Meric-Bernstam, F. & Gonzalez-Angulo, A.M. Targeting the mTOR signaling network for cancer therapy. *J. Clin. Oncol.* **27**, 2278–2287 (2009).

ONLINE METHODS

Whole-genome sequencing. High molecular weight DNA was extracted from freshly frozen tumor tissue and lymphocytes. DNA was fragmented using an ultrasonic solubilizer (Covaris) using a combination of quick bursts (20% duty, 5 intensity with 200 cycles per burst for 5 s) and sonication (10% duty, 5 intensity with 200 cycles per burst for 120 s) for the short fragment DNA library. DNA of the appropriate size was gel purified to exclude any inappropriate DNA fusions during library construction. The short fragment DNA libraries were generated using a paired-end DNA sample prep kit (Illumina) following the manufacturer's protocols. The concentration of the libraries was quantified using a Bioanalyzer (Agilent Technologies); 4~8 pM/lane of DNA was applied to the flow cell, and paired-end sequencing was performed using the GAIIx sequencer (Illumina).

Whole-exome capture sequencing. Whole-exome capture sequencing was performed using the SureSelect Target Enrichment System (Agilent Technologies) in accordance with the manufacturer's protocol with slight modifications. Briefly, the same Illumina sequence libraries as those prepared for the whole-genome sequence were amplified with six cycles of PCR, and then 500 ng of the amplified libraries was hybridized with the capture probes for 24 h. The hybridized sequence libraries were collected and further amplified with 14 cycles of PCR. We generated 51-nucleotide–long paired-end reads using the GAIIx sequencer (Illumina). We used five lanes of a paired-end flow cell for each sample.

Bioinformatics (Supplementary Fig. 11). *Sequence alignment to the human genome and removal of PCR duplications.* Paired-end reads were aligned to the human reference genome (hg18, NCBI Build 36.1) using Burrows-Wheeler Aligner (BWA) (version 0.4.9)[25]. Because there were duplicated reads which were generated during the PCR amplification process, paired-end reads that aligned to the same genomic positions were removed using SAMtools (version 0.1.5c)[26] and a program developed in house. We removed 12.5% (14.6/117.1 Gbp) of the aligned reads for tumor and 7.1% (6.1/86.3 Gbp) for lymphocytes.

Detection of somatic single nucleotide variations (SNVs) **(Supplementary Fig. 12).** Based on the genotyping data from two SNP arrays, appropriate thresholds for base quality, mapping quality and frequency of non-reference alleles were determined to obtain the highest confidence calls for SNV detection (**Supplementary Table 4**). To predict somatic SNVs, the alignment results were classified, and three datasets were constructed. Dataset 1 included paired-end reads with both ends aligned uniquely and with proper spacing and orientation. Dataset 2 included paired-end reads that aligned uniquely for at least one read and with proper spacing and orientation of the reads. Dataset 3 included dataset 2 and paired-end reads for which both ends aligned uniquely but with improper spacing or orientation or both. Dataset 1 likely contains false positive somatic SNVs because of the low sequence depth of the lymphocyte genome, and dataset 3 likely contains false positives due to misalignments of the sequence reads. To reduce the number of false positives, the following filters were applied to these three datasets, and concordant somatic SNVs among the three datasets were selected: (i) a mapping quality score of 20 was used as a cutoff value for read selection; (ii) base quality scores of 10 and 15 were used as cutoff values for base selection for the tumor and lymphocyte genomes, respectively; (iii) SNVs were selected when the frequency of the non-reference allele was at least 15% in the tumor genome and 5% in the lymphocyte genome; (iv) SNVs located within 5 bp from a potential insertion or deletion were discarded; (v) SNVs with a root mean square mapping quality score of the reads covering the SNV less than 40 were discarded; (vi) when there were three or more SNVs within any 10-bp window, all of them were discarded; (vii) SNVs with a consensus quality score less than 20 as calculated by SAMtools (version 0.1.5c) were discarded; (viii) when a base with a consensus quality score less than 20 was located within 3-bp on either side of a SNV, the SNV was discarded; (ix) for the tumor genome, SNVs found in at least two sequence reads with the same SNV were selected; (x) for the lymphocyte genome, SNVs covered by at least six sequence reads were selected; and (xi) the repetitive regions within 1 Mb of a centromeric or telomeric sequence gap were excluded. By comparing the predicted nucleotide variations in the tumor and lymphocyte genomes, somatic SNVs which occurred only in the tumor genome were identified. If somatic SNVs were not covered in the lymphocyte genome by at least six sequence reads, they were discarded.

Using this approach, 66 non-synonymous and 24 synonymous somatic SNVs in protein-coding regions were predicted. These 90 substitutions were examined by Sanger sequencing of both the tumor and lymphocyte genomes, and 81 of them were validated as somatic mutations. Of the remaining nine substitutions, three could not be amplified by PCR, four could not be sequenced because of the surrounding repetitive sequences, and two could not be validated likely because they were located in highly homologous segmentally duplicated or processed pseudogene regions, suggesting a high prediction accuracy (specificity, 81/83 = 97.6%) for our approach for detecting somatic SNVs in protein-coding regions. An additional 36 non-synonymous somatic SNVs were also predicted using only dataset 3 and filtering methods (i–iv) (less stringent filtering condition). Five of these SNVs were not validated and 30 of them were found to be germline variations by Sanger sequencing, and only the one remaining was validated as a somatic mutation. These findings suggest that our filtering method (stringent condition) effectively removed false-positive somatic SNVs.

Detection of somatic structural alterations. To detect structural alterations, paired-end reads for which both ends aligned uniquely to the human reference genome, but with improper spacing or orientation or both, were used. First, paired-end reads were selected based on the following filtering conditions: (i) sequence reads with mapping quality scores greater than 37; and (ii) sequence reads aligned with two mismatches or less.

Rearrangements were then identified using the following analytical conditions: (i) 'clusters' which included reads aligned within the maximum insert distance were constructed from the forward and reverse alignments, respectively (two reads were allocated to the same cluster if their end positions were not further apart than the maximum insert distance); (ii) clusters whose distance between the leftmost and rightmost reads were greater than the maximum insert distance were discarded; (iii) paired-end reads were selected if one end sequence was allocated in the 'forward cluster' and the other end was allocated in the 'reverse cluster' (we called these 'forward cluster and reverse cluster' paired clusters); (iv) if a cluster overlapped another cluster, all of the overlapping paired-clusters were discarded; (v) for the tumor genome, rearrangements (paired-clusters) predicted by at least four paired-end reads which included at least one paired-end read perfectly matched to the human reference genome were selected; and (vi) for the lymphocyte genome, rearrangements (paired clusters) predicted by at least one paired-end read were selected. By comparing the predicted rearrangements in the tumor and lymphocyte genomes, somatic rearrangements that were only detected in the tumor genome were identified.

Lastly, rearrangements predicted due to variations in the analyzed genomes were removed. For this analysis, paired-end reads contained in paired clusters were aligned to the human reference genome using the BLASTN program (see URLs). If one end sequence was aligned to the region of paired clusters (the flanking region of the rearrangement breakpoint) and the other end was aligned with proper spacing and orientation, the rearrangement was removed. An expectation value of 1,000 was used as a cutoff value for BLASTN so that paired-end reads with low similarity to the human reference genome could also be aligned.

Using this method, 33 somatic rearrangements were predicted and 22 of these were validated by Sanger sequencing of the rearrangement breakpoints in both the tumor and lymphocyte genomes.

Exome capture sequence analysis. To analyze the capture sequencing data, the Illumina sequencing pipeline version 1.4 and in-house programs were used. The sequence reads were mapped to the human reference sequence (NCBI Build 36.3) using GERALD (Illumina), and only high-quality ('pass filter') reads with base-call quality scores more than ten were used for SNV detection.

doi:10.1038/ng.804

SNVs were determined using the frequency (>20%) of the highest non-reference base call with a read depth greater than 20×.

Other molecular analyses. SNP genotyping and copy number detection were determined using the Affymetrix Mapping 500K Array, the Agilent Human Genome CGH microarray and the Illumina Human 610-Quad BeadChip system. Gene expression levels of the tumor were measured using the Agilent Whole Human Genome Oligo Microarray. Wild-type and mutant allele frequencies were determined using the Digital PCR system.

Detailed experimental methods and additional bioinformatics procedures are described in **Supplementary Note**. The somatic substitutions and insertions/deletions found are listed in **Supplementary Tables 5–9**.

25. Li, H. & Durbin, R. Fast and accurate short read alignment with Burrows-Wheeler Transform. *Bioinformatics* **25**, 1754–1760 (2009).
26. Li, H. *et al.* The Sequence alignment/map (SAM) format and SAMtools. *Bioinformatics* **25**, 2078–2079 (2009).

JJCO Japanese Journal of Clinical Oncology

Jpn J Clin Oncol 2011;41(6)770–775
doi:10.1093/jjco/hyr037
Advance Access Publication 1 April 2011

Transcatheter Arterial Infusion Chemotherapy with a Fine-powder Formulation of Cisplatin for Advanced Hepatocellular Carcinoma Refractory to Transcatheter Arterial Chemoembolization

Satoru Iwasa[1], Masafumi Ikeda[2,*], Takuji Okusaka[1], Hideki Ueno[1], Chigusa Morizane[1], Kohei Nakachi[2], Shuichi Mitsunaga[2], Shunsuke Kondo[1], Atsushi Hagihara[1], Satoshi Shimizu[2], Mitsuo Satake[3] and Yasuaki Arai[4]

[1]Hepatobiliary and Pancreatic Oncology Division, National Cancer Center Hospital, Tokyo, [2]Division of Hepatobiliary and Pancreatic Oncology, National Cancer Center Hospital East, Chiba, [3]Division of Diagnostic Radiology, National Cancer Center Hospital East, Chiba and [4]Division of Diagnostic Radiology, National Cancer Center Hospital, Tokyo, Japan

*For reprints and all correspondence: Masafumi Ikeda, Division of Hepatobiliary and Pancreatic Oncology, National Cancer Center Hospital East, 6-5-1 Kashiwanoha, Kashiwa, Chiba 277-8577, Japan. E-mail: masikeda@east.ncc.go.jp

Received November 14, 2010; accepted February 25, 2011

Objective: The aim of this study was to assess the safety and efficacy of transcatheter arterial infusion chemotherapy using a fine-powder formulation of cisplatin for patients with advanced hepatocellular carcinoma refractory to transcatheter arterial chemoembolization.
Methods: We retrospectively examined the data of 84 consecutive patients with transcatheter arterial chemoembolization-refractory hepatocellular carcinoma who underwent transcatheter arterial infusion chemotherapy with a fine-powder formulation of cisplatin. Cisplatin was administered at the dose of 65 mg/m^2 into the feeding artery of the hepatocellular carcinoma. The treatment was repeated every 4–6 weeks, until the appearance of evidence of tumor progression or of unacceptable toxicity.
Results: Of the 84 patients, one patient (1.2%) showed complete response and two patients (2.4%) showed partial response, representing an overall response rate of 3.6% (95% confidence interval, 0.7–10.1). Of the remaining, 38 patients (45.2%) showed stable disease and 41 (48.8%) showed progressive disease. The median overall survival, 1-year survival rate and median progression-free survival in the entire subject population were 7.1 months, 27% and 1.7 months, respectively. Major Grade 3 or 4 adverse events included thrombocytopenia in 12 patients (14%) and elevation of the serum aspartate aminotransferase in 33 patients (39%). The gastrointestinal toxicities were mild and reversible.
Conclusions: Transcatheter arterial infusion chemotherapy using a fine-powder formulation of cisplatin appears to have only modest activity, although the toxicity was also only mild, in patients with transcatheter arterial chemoembolization-refractory hepatocellular carcinoma.

Key words: hepatocellular carcinoma – transcatheter arterial infusion chemotherapy – cisplatin – transcatheter arterial chemoembolization

INTRODUCTION

Hepatocellular carcinoma (HCC) is treated by one or more of a wide variety of treatment options available, depending on the tumor characteristics, including the number and size of tumors, and the presence/absence of tumor thrombosis and extrahepatic metastases (1,2). In patients with early-stage HCC, curative therapies can be applied, including resection, liver transplantation or local ablation therapy. However, the prognosis of patients with HCC is still unsatisfactory, mainly because of the high frequency of recurrence post-therapy (3–9). Transcatheter arterial chemoembolization (TACE) has been performed for unresectable advanced HCC in patients who are unsuitable candidates for local ablation therapy or surgical treatment. To date, nine randomized control trials

(RCTs) of transcatherter arterial embolization or TACE versus best supportive care have been reported (10–18). Three of these RCTs and two meta-analyses have demonstrated a survival benefit of this treatment modality in HCC patients (10,16,17,19,20). On the basis of these results, TACE has been the most commonly employed treatment modality in patients with unresectable advanced HCC, especially those with intermediate-stage disease, who are unsuitable candidates for local ablation therapy (21). However, unfortunately, the disease eventually progresses to becoming refractory to TACE.

Transcatheter arterial infusion chemotherapy (TAI) could be expected to have better antitumor efficacy and lesser toxicity than systemic chemotherapy, because it is associated with only a local increase in the concentrations of anticancer drugs, and therefore, a lower incidence of systemic adverse effects. The reported response rates to TAI with a single agent vary in the range of 9–33% (22–25), and those to TAI using combination regimens vary in the range of 44–73% (26–29). Thus, TAI has high antitumor activity and is widely used in clinical practice, especially in Japan, although no survival benefit has been established yet, because no randomized studies of TAI have been conducted until date.

Cisplatin for Intra-arterial Injection (IA-call®, Nippon Kayaku Co., Ltd) is a powder formulation and represents an improvement over the standard liquid type of cisplatin formulation for intra-arterial administration. Since the solubility of this agent is 2.86 times higher than that of standard cisplatin, the injection time can be shortened. In a clinical study of this agent for advanced HCC, a favorable tumor response rate of 33.8% was reported (25), and this agent was approved for use in the treatment of HCC by the Ministry of Health, Labour and Welfare of Japan, in July 2004. However, it has not been clarified whether this agent might also be effective for TACE-refractory HCC. Therefore, we conducted a retrospective investigation of the efficacy and safety of TAI using cisplatin in patients with HCC refractory to TACE.

PATIENTS AND METHODS

Patients and Treatment

From July 2004 to September 2008, 84 consecutive patients with TACE-refractory HCC underwent TAI using cisplatin at the National Cancer Center Hospital, Tokyo, or the National Cancer Center Hospital East, Chiba, Japan. TACE-refractory tumors were defined as those showing an increase in size or <25% reduction in size of the hypervascular lesions visualized on dynamic computed tomography (CT) and/or magnetic resonance imaging (MRI) at 1 month after TACE (30).

TAI was performed by introducing a catheter into the proper, right or left hepatic artery, or another feeding artery by the Seldinger technique, and injecting cisplatin at the dose of 65 mg/m^2 over 20–40 min. Until the appearance of evidence of tumor progression and/or of unacceptable toxicity, the treatment was repeated every 4–6 weeks for up to six cycles. Antiemetic prophylaxis with a 5-hydroxytryptamine3 antagonist (granisetron 1 mg) plus dexamethasone 8 mg was used at the physician's discretion. Patients received adequate hydration for protection against cisplatin-induced renal dysfunction, and the urine output was carefully monitored, especially during the first 3 days after intra-arterial administration of cisplatin, and intravenous furosemide was administered if the output was judged to be inadequate. In principle, the cisplatin dose was reduced if the patient's creatinine clearance decreased to below 50 ml/min.

This retrospective study was conducted with the approval of the Institutional Review Board of the National Cancer Center and conducted in accordance with the ethical principles stated in Japanese ethics guidelines for epidemiologic studies.

Response and Toxicity Evaluations

The antitumor effect was evaluated by dynamic CT and/or MRI performed 1 month after each treatment cycle, and after the completion of six cycles, follow-up examinations were performed every 1–3 months. Responses were evaluated according to the Response Evaluation Criteria in Solid Tumors (RECIST) (31). The best overall response was recorded for each patient. Progression-free survival was defined as the interval between the date of the initial TAI treatment using cisplatin and either the date of documentation of disease progression (either radiologic or symptomatic progression) or the date of death owing to any cause. Overall survival was measured from the date of the initial TAI treatment using cisplatin to the date of death or last follow-up. Survival curves were estimated using the Kaplan–Meier method. Toxicities were assessed using the Common Terminology Criteria for Adverse Events, version 3.0. Statistical analyses were performed using Dr SPSS II (SPSS Japan Inc., Tokyo, Japan).

RESULTS

Patient Characteristics

The baseline characteristics of the 84 patients enrolled in this study are shown in Table 1. The diagnosis of HCC was made either by histologic examination (44 patients, 52%), or distinctive findings on CT, MRI and/or angiography associated with elevated serum levels of α-fetoprotein or protein induced by vitamin K antagonist II (40 patients, 48%). Of the total, 42 patients each were classified as the Child–Pugh classes A and B, whereas there were no patients of the Child–Pugh class C. Twenty-six patients (31%) had tumor thrombosis in the main and/or first portal vein. Prior therapies other than TACE were hepatectomy (37 patients, 44%), local ablation therapy (33 patients, 39%), TAI (13 patients, 15%) and systemic chemotherapy (10 patients, 12%) with non-platinum-containing regimens. The median number of

Table 1. Patient characteristics ($n = 84$)

Age, median (range)	68 (37–82)
Gender, *n* (%)	
Male	69 (82)
Female	15 (18)
ECOG performance status, *n* (%)	
0	56 (67)
1	26 (31)
2	0 (0)
3	2 (2)
T factor[a]	
T1	2 (2)
T2	34 (40)
T3a	17 (20)
T3b	31 (37)
Portal vein tumor thrombosis, *n* (%)	
Present	26 (31)
Absent	58 (69)
Ascites, *n* (%)	
Present	24 (29)
Absent	60 (71)
Hepatitis virus marker status, *n* (%)	
HBsAg-positive	12 (14)
HCVAb-positive	55 (65)
Child–Pugh class, *n* (%)	
A	42 (50)
B	42 (50)
Number of previous TACE sessions	
Median (range)	4 (1–17)
Reason for TACE-refractory disease, *n* (%)	
Progressive disease	69 (82)
Stable disease (under 25% decrease)	15 (18)
AFP (ng/dl)	
Median (range)	660.2 (1.7–4 06 500)
PIVKA II (mAU/ml)	
Median (range)	600 (11–96 390)

ECOG, Eastern Cooperative Oncology Group; HBsAg, hepatitis B surface antigen; HCVAb, hepatitis C virus antibody; TACE, transcatheter arterial chemoembolization; AFP, α-fetoprotein; PIVKA, protein induced by vitamin K antagonist.
[a]T factor was evaluated according to Sobin et al. (32).

previous sessions of TACE was 4 (range 1–17), and the median period from the first TACE to the date on which the tumors were judged to be TACE-refractory was 15.8 months (range 1.0–78.0). The anticancer agents used for the previous TACE sessions were epirubicin in 79 patients, adriamycin in 17 patients and mitomycin C in 5 patients.

Treatment Delivery and Efficacy

In total, 167 cycles of TAI were administered to the 84 patients, with a median of one cycle (range 1–7) per patient. The median cisplatin dose per treatment session was 100 mg (range 50–135). A total of 83 patients received the standard dose of cisplatin in the first session, and the remaining one patient required a 50% reduction in the dose of cisplatin even from the first treatment cycle because of pre-existing renal dysfunction.

Of the study population, one patient showed complete response and two showed partial response, representing an overall response rate of 3.6% [95% confidence interval (CI), 0.7–10.1]. Stable disease was noted in 38 patients and progressive disease in 41 patients. The remaining two patients were not evaluable as they were lost to follow-up. After treatment discontinuation, 50 (60%) patients received supportive care only, 32 (38%) received additional anticancer therapy and 2 (2%) were lost to follow-up. The additional anticancer therapies were TACE with epirubicin or mitomycin in 18 patients, TAI using non-platinum drugs in 7 patients (including 5-fluorouracil with systemic interferon in 3 patients, epirubicin in 3 patients and zinostatin-stimalamer in 1 patient), systemic chemotherapy in 5 patients (including S-1, i.e. a mixture of tegafur, 5-chloro-2,4-dihydropyrimidine and potassium oxonate, in 3 patients and uracil–tegafur plus mitoxantrone in 2 patients) and immunotherapy in 2 patients. By the time of the analysis, except for eight patients who were still alive but showed disease progression, all of the patients had died. The median progression-free survival was 1.7 months (95% CI, 1.1–2.3) and the median overall survival was 7.1 months (95% CI, 4.9–9.3), with a l-year survival rate of 27% (Fig. 1).

Adverse Events

Data of all 84 patients were analyzed for adverse events. The adverse events are summarized in Table 2. In regard to the hematologic adverse events, thrombocytopenia was the most common, with 12 (14%) patients developing Grade 3 or 4 thrombocytopenia; however, none of the patients required platelet transfusions. Grade 3 or 4 leukopenia and neutropenia occurred in only 6 and 4% of the patients, respectively. There were no events of febrile neutropenia.

The main non-hematologic adverse events were elevation of the serum aspartate aminotransferase (AST) and serum alanine aminiotransferase (ALT). Grade 3 or 4 elevation of the AST and ALT was observed in 33 (39%) and 5 (6%) patients, respectively. Gastrointestinal adverse events, such as nausea, vomiting and anorexia, were frequently observed after intra-arterial administration of cisplatin, but most were transient and manageable with appropriate medical treatment, such as antiemetic drug administration and intravenous hydration. There was no serious renal toxicity. Four patients died within 30 days of the last treatment session: two of disease progression, one of acute coronary syndrome,

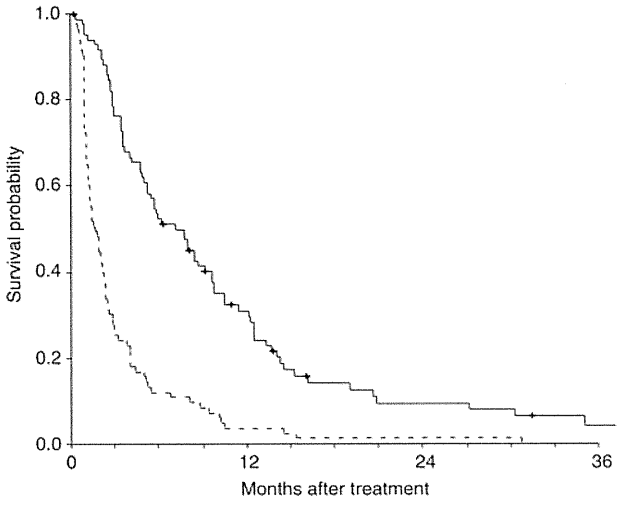

Figure 1. Overall survival (continuous line) and progression-free survival (dotted line) in the 84 patients. The marks on the curve represent censored cases.

Table 2. Adverse events

	No. of patients				Gr 3/4 (%)
	Gr 1	Gr 2	Gr 3	Gr 4	
Hematologic toxicity					
Leukocytopenia	30	29	5	0	6.0
Neutropenia	11	24	3	0	3.6
Anemia	55	18	6	1	8.3
Thrombocytopenia	36	22	12	0	14.3
Non-hematologic toxicity					
Anorexia	45	16	3	0	3.6
Nausea	40	9	3	0	3.6
Vomiting	11	6	0	0	0
Fatigue	59	11	3	0	3.6
Diarrhea	3	1	0	0	0
Constipation	20	0	0	0	0
Hypoalbuminemia	38	41	1	0	1.2
Elevated serum total bilirubin	28	33	4	1	6.0
Elevated serum aspartate aminotransferase	20	26	31	2	39.3
Elevated serum alanine aminotransferase	37	30	4	1	6.0
Elevated serum alkaline phosphatase	53	15	1	0	1.2
Elevated serum creatinine	12	1	0	0	0

Gr, grade.

showing no causal relationship with the treatment, and the remaining one due to known pulmonary artery tumor embolism.

DISCUSSION

In the current study, the response rate to TAI using cisplatin was only 3.6% in patients with TACE-refractory HCC. Moreover, the median progression-free survival of only 1.7 months was extremely disappointing. The efficacy of TAI using cisplatin for advanced HCC limited to TACE-refractory tumors was much worse than that reported from a previous Phase II study in patients with advanced HCC (response rate, 33.8%) (25). One possible explanation for this discrepancy in the response rate may be the differences in the characteristics of the enrolled patients between the two studies. Most patients in the previous Phase II trial were TACE-naïve, whereas only patients with TACE-refractory disease were included in the current study. In our previous study (30), TAI using epirubicin was reported to have unfavorable efficacy in a subset of patients with TACE-refractory HCC (response rate, 5%). When HCC is treated by TACE and/or becomes resistant to TACE, it might acquire resistance to cytotoxic agents, such as cisplatin or epirubicin. Furthermore, to select suitable candidates for this treatment, the predictive factors for disease control and survival for more than 12 months were also investigated, but could not be clarified (data not shown). Therefore, TAI using cisplatin or epirubicin cannot be recommended at present for this patient population in clinical practice.

Recently, systemic chemotherapy has become an important treatment modality for advanced HCC, because two RCTs (the SHARP trial and the Asia-pacific trial) of sorafenib versus placebo demonstrated significantly improved time-to-progression and overall survival in the drug-treated group, although sorafenib yielded a far-from-satisfactory response rate of only 2.3–3.3% (33,34). On the basis of the results of these RCTs, sorafenib is acknowledged as a standard agent for systemic chemotherapy in patients with advanced HCC. The efficacy of sorafenib for advanced HCC refractory to TACE has not yet been clarified, but in both of the aforementioned studies, the results of exploratory subgroup analyses in patients treated previously by TACE were reported. In the subset of patients with a previous history of treatment by TACE in the SHARP trial, the disease control rate (DCR) was significantly greater in the patients who were treated with sorafenib (44.2%) than in those who had received placebo (34.4%) (35). In addition, a trend towards a beneficial effect of sorafenib was also observed in relation to the median overall survival in this subpopulation of patients {11.9 vs. 9.9 months [hazard ratio (HR), 0.75; 95% CI, 0.49–1.14]}. In the Asia-pacific trial, 41% of the enrolled patients had a previous history of undergoing TACE. The DCR for sorafenib (24.6%) in these patients was higher than that for placebo (9.1%) (36). Moreover, a tendency [HR for death was 0.84 (95% CI, 0.52–1.36)] towards favorable overall survival was also noted in the HCC patients with a previous history of TACE treated with sorafenib when compared with that in the same subpopulation of patients who received placebo. Sorafenib appeared to benefit patients with

advanced HCC, regardless of whether or not they had previously been treated by TACE. Thus, molecular-targeted agents, including sorafenib, which exhibit mechanisms of action different from those of cytotoxic agents, may be superior for the treatment of HCC refractory to TACE. Therefore, patients with TACE-refractory HCC are receiving new molecular-targeted agents in clinical trials, and sorafenib is used as the standard agent for the treatment of advanced HCC in clinical practice.

In the current study, the most common Grade 3 and 4 adverse events were elevated AST, thrombocytopenia and anemia, which frequently also reflected the underlying cirrhosis. In terms of the gastrointestinal toxicities, only 4% of the patients experienced Grade 3 anorexia and nausea, and the symptoms resolved within a few days. Thus, the gastrointestinal toxicities were mild and manageable in the current study. There was no need for dose reduction or discontinuation of cisplatin on account of development of toxicities, except in one patient each with Grade 2 elevation of the serum creatinine and Grade 2 fatigue. Thus, advanced HCC patients showed good overall tolerability to TAI using cisplatin, which has also been reported to show favorable efficacy in these patients (25); in our study confined to TACE-refractory patients, however, the treatment showed only modest antitumor activity. TAI using cisplatin may therefore be easy to administer in combination with some molecular-targeted agents, such as sorafenib, since its toxicity is generally mild and its toxicologic profile is distinct from that of sorafenib.

In conclusion, TAI using cisplatin appeared to have only modest activity against TACE-refractory HCC, although this treatment was feasible and well tolerated. Further development of novel treatments is necessary to improve the prognosis of patients with TACE-refractory HCC.

Acknowledgements

We thank the office administrators of the Hepatobiliary and Pancreatic Oncology Division at both institutions for their support in the preparation of this manuscript (Ms Kayo Takei, Keiko Kondo and Rubi Mukouyama).

Funding

This study was supported in part by a Grant-in-Aid for Cancer Research from the Ministry of Health, Labour and Welfare, Japan.

Conflict of interest statement

None declared.

References

1. Llovet JM. Updated treatment approach to hepatocellular carcinoma. *J Gastroenterol* 2005;40:225–35.
2. Llovet JM, Bruix J. Novel advancements in the management of hepatocellular carcinoma in 2008. *J Hepatol* 2008;48:S20–37.
3. Belghiti J, Panis Y, Farges O, Benhamou JP, Fekete F. Intrahepatic recurrence after resection of hepatocellular carcinoma complicating cirrhosis. *Ann Surg* 1991;214:114–7.
4. Figueras J, Jaurrieta E, Valls C, Benasco C, Rafecas A, Xiol X, et al. Survival after liver transplantation in cirrhotic patients with and without hepatocellular carcinoma: a comparative study. *Hepatology* 1997;25:1485–9.
5. Lesurtel M, Müllhaupt B, Pestalozzi BC, Pfammatter T, Clavien PA. Transarterial chemoembolization as a bridge to liver transplantation for hepatocellular carcinoma: an evidence-based analysis. *Am J Transplant* 2006;6:2644–50.
6. Porrett PM, Peterman H, Rosen M, Sonnad S, Soulen M, Markmann JF, et al. Lack of benefit of pre-transplant locoregional hepatic therapy for hepatocellular cancer in the current MELD era. *Liver Transpl* 2006;12:665–73.
7. Rossi S, Di Stasi M, Buscarini E, Quaretti P, Garbagnati F, Squassante L, et al. Percutaneous RF interstitial thermal ablation in the treatment of hepatic cancer. *Am J Roentgenol* 1996;167:759–68.
8. Ishii H, Okada S, Nose H, Okusaka T, Yoshimori M, Takayama T, et al. Local recurrence of hepatocellular carcinoma after percutaneous ethanol injection. *Cancer* 1996;77:1792–6.
9. Livraghi T, Giorgio A, Marin G, Salmi A, de Sio I, Bolondi L, et al. Hepatocellular carcinoma and cirrhosis in 746 patients: long-term results of percutaneous ethanol injection. *Radiology* 1995;197:101–8.
10. Lin DY, Liaw YF, Lee TY, Lai CM. Hepatic arterial embolization in patients with unresectable hepatocellular carcinoma—a randomized controlled trial. *Gastroenterology* 1988;94:453–6.
11. Pelletier G, Roche A, Ink O, Anciaux ML, Derhy S, Rougier P, et al. A randomized trial of hepatic arterial chemoembolization in patients with unresectable hepatocellular carcinoma. *J Hepatol* 1990;11:181–4.
12. Madden MV, Krige JE, Bailey S, Beningfield SJ, Geddes C, Werner ID, et al. Randomised trial of targeted chemotherapy with lipiodol and 5-epidoxorubicin compared with symptomatic treatment for hepatoma. *Gut* 1993;34:1598–600.
13. Groupe d'Etude et de Traitement du Carcinome Hepatocellulaire. A comparison of lipiodol chemoembolization and conservative treatment for unresectable hepatocellular carcinoma. *N Engl J Med* 1995;332:1256–61.
14. Pelletier G, Ducreux M, Gay F, Luboinski M, Hagège H, Dao T, et al. Treatment of unresectable hepatocellular carcinoma with lipiodol chemoembolization: a multicenter randomized trial. Groupe CHC. *J Hepatol* 1998;29:129–34.
15. Bruix J, Llovet JM, Castells A, Montañá X, Brú C, Ayuso MC, et al. Transarterial embolization versus symptomatic treatment in patients with advanced hepatocellular carcinoma: results of a randomized, controlled trial in a single institution. *Hepatology* 1998;27:1578–83.
16. Lo CM, Ngan H, Tso WK, Liu CL, Lam CM, Poon RT, et al. Randomized controlled trial of transarterial lipiodol chemoembolization for unresectable hepatocellular carcinoma. *Hepatology* 2002;35:1164–71.
17. Llovet JM, Real MI, Montaña X, Planas R, Coll S, Aponte J, et al., Barcelona Liver Cancer Group. Arterial embolisation or chemoembolisation versus symptomatic treatment in patients with unresectable hepatocellular carcinoma: a randomised controlled trial. *Lancet* 2002;359:1734–39.
18. Doffoël M, Bonnetain F, Bouché O, Vetter D, Abergel A, Fratté S, et al. Multicentre randomised phase III trial comparing Tamoxifen alone or with Transarterial Lipiodol Chemoembolisation for unresectable hepatocellular carcinoma in cirrhotic patients (Fédération Francophone de Cancérologie Digestive 9402). *Eur J Cancer* 2008;44:528–38.
19. Llovet JM, Bruix J. Systematic review of randomized trials for unresectable hepatocellular carcinoma: chemoembolization improves survival. *Hepatology* 2003;37:429–42.
20. Camma C, Schepis F, Orlando A, Albanese M, Shahied L, Trevisani F, et al. Transarterial chemoembolization for unresectable hepatocellular carcinoma: meta-analysis of randomized controlled trials. *Radiology* 2002;224:47–54.

21. Llovet JM, Burroughs A, Bruix J. Hepatocellular carcinoma. *Lancet* 2003;362:1907–17.
22. Tzoracoleftherakis EE, Spiliotis JD, Kyriakopoulou T, Kakkos SK. Intra-arterial versus systemic chemotherapy for non-operable hepatocellular carcinoma. *Hepatogastroenterology* 1999;46:1122–5.
23. Ikeda M, Okusaka T, Ueno H, Morizane C, Iwasa S, Hagihara A, et al. Hepatic arterial infusion chemotherapy with epirubicin in patients with advanced hepatocellular carcinoma and portal vein tumor thrombosis. *Oncology* 2007;72:188–93.
24. Furuse J, Ikeda M, Okusaka T, Nakachi K, Morizane C, Ueno H, et al. A phase II trial of hepatic arterial infusion chemotherapy with cisplatin for advanced hepatocellular carcinoma with portal vein tumor thrombosis. 2008 ASCO Annual Meeting Proceedings (Post-Meeting Edition), abstr 15556.
25. Yoshikawa M, Ono N, Yodono H, Ichida T, Nakamura H. Phase II study of hepatic arterial infusion of a fine-powder formulation of cisplatin for advanced hepatocellular carcinoma. *Hepatol Res* 2008;38:474–83.
26. Ando E, Tanaka M, Yamashita F, Kuromatsu R, Yutani S, Fukumori K, et al. Hepatic arterial infusion chemotherapy for advanced hepatocellular carcinoma with portal vein tumor thrombosis: analysis of 48 cases. *Cancer* 2002;95:588–95.
27. Ota H, Nagano H, Sakon M, Eguchi H, Kondo M, Yamamoto T, et al. Treatment of hepatocellular carcinoma with major portal vein thrombosis by combined therapy with subcutaneous interferon-alpha and intra-arterial 5-fluorouracil; role of type I interferon receptor expression. *Br J Cancer* 2005;93:557–64.
28. Obi S, Yoshida H, Toune R, Unuma T, Kanda M, Sato S, et al. Combination therapy of intraarterial 5-fluorouracil and systemic interferon-alpha for advanced hepatocellular carcinoma with portal venous invasion. *Cancer* 2006;106:1990–7.
29. Sakon M, Nagano H, Dono K, Nakamori S, Umeshita K, Yamada A, et al. Combined intraarterial 5-fluorouracil and subcutaneous interferon-alpha therapy for advanced hepatocellular carcinoma with tumor thrombi in the major portal branches. *Cancer* 2002;94:435–42.
30. Tanaka T, Ikeda M, Okusaka T, Ueno H, Morizane C, Ogura T, et al. A phase II trial of transcatheter arterial infusion chemotherapy with an epirubicin-Lipiodol emulsion for advanced hepatocellular carcinoma refractory to transcatheter arterial embolization. *Cancer Chemother Pharmacol* 2008;61:683–8.
31. Therasse P, Arbuck SG, Eisenhauer EA, Wanders J, Kaplan RS, Rubinstein L, et al. New guidelines to evaluate the response to treatment in solid tumors. *J Natl Cancer Inst* 2000;92:205–16.
32. Sobin LH, Gospodarowicz MK, Wittekind C. *International Union Against Cancer (UICC) TNM Classification of Malignant Tumours*. 7th edn. Oxford, UK: Wiley-Blackwell 2009.
33. Llovet JM, Ricci S, Mazzaferro V, Hilgard P, Gane E, Blanc JF, et al. Sorafenib in advanced hepatocellular carcinoma. *N Engl J Med* 2008;359:378–90.
34. Cheng AL, Kang YK, Chen Z, Tsao CJ, Qin S, Kim JS, et al. Efficacy and safety of sorafenib in patients in the Asia-Pacific region with advanced hepatocellular carcinoma: a phase III randomised, double-blind, placebo-controlled trial. *Lancet Oncol* 2009;10:25–34.
35. Galle PR, Blanc J, Van Laethem JL, Marrero J, Beaugrand M, Moscovioi M, et al. Efficacy and safety of sorafenib in patients with advanced hepatocellular carcinoma and prior anti-tumor therapy: a sub-analysis from the SHARP trial. 43rd Annual Meeting of the European Association for the Study of the Liver (EASL 2008). Milan, Italy, 23–27 April 2008.
36. Tak WY, Yu S, Tsao CJ, Yang TS, Kim JS, Qin S, et al. Impact of prior TACE/TAE on the efficacy and safety of sorafenib in patients with advanced hepatocellular carcinoma (HCC) form the Asia-Pacific region. *J Hepatol* 2009;50:S301.

	L I V	2 7 6 3	B	Dispatch: 24.1.12	Journal: LIV	CE: Ulagammal
	Journal Name	Manuscript No.		Author Received:	No. of pages: 2	PE: Sangeetha

Liver International ISSN 1478-3223

Letter to the Editor

DOI:10.1111/j.1478-3231.2012.02763.x

Incidence of hepatocellular carcinoma and response to interferon therapy in HCV-infected patients: effect of factors associated with the therapeutic response and incidence of HCC

To the Editor:

Several previous studies reported a significantly lower incidence of hepatocellular carcinoma (HCC) in hepatitis C virus (HCV)-infected patients who showed sustained virological response (SVR) to or relapsed on antiviral therapy with interferon (IFN) or peginterferon (PEG-IFN), with or without ribavirin compared with no responders (NR; i.e. partial response, viral breakthrough, or null-response) (1, 2). The reduction in HCC incidence was especially marked in patients with SVR. These results have been taken as evidence that antiviral therapy has an effect of suppressing the development of HCC.

Recently reported viral and host factors that are strongly associated with response to anti-HCV therapy (3, 4) may also be associated with the pathogenesis of HCC. Amino acid substitution in the HCV core region, a viral factor reportedly associated with response to PEG-IFN and ribavirin therapy (3), is also associated with the development of HCC (5). Regarding host factors associated with response to anti-HCV therapy (4), genetic polymorphisms near the *IL28* gene are reportedly associated with hepatic steatosis (6) and interact with amino acid substitutions in the HCV core region (7), both of which are associated with the development of HCC (5, 8).

We analysed the incidence of HCC in 448 patients who completed anti-HCV therapy with IFN or PEG-IFN and in whom the genetic polymorphisms near *IL28B* gene were analysed after the approval of the hospital ethics committee and obtaining written informed consent. We found significant differences in the incidence of HCC between patients with SVR ($n = 247$), relapse ($n = 122$), and NR ($n = 79$) (Fig. 1A, $P < 0.0001$ by Log-rank test). However, the prevalence of patients having TT genotype at rs8099917 near the *IL28B* gene, which is associated with favourable response to anti-HCV therapy, was significantly lower in patients with NR (SVR, 85.8%; relapse, 80.3%; NR, 39.2%; $P < 0.0001$ by Chi-square test). In addition, we found significant differences in the incidence of HCC also according to the genotype of rs8099917 (Fig. 1B, $P = 0.0156$). Although multivariate analysis using Cox proportional hazard model including age, gender, HCV genotype, and the outcome of therapy, but not *IL28B* polymorphisms identified SVR ($P = 0.0083$) and relapse ($P = 0.0493$) as independent factors that were associated with lower incidence of HCC, it failed to detect an independent factor that was associated with the incidence of HCC when *IL28B* polymorphisms were included. These results suggested that the previously reported differences in the incidence of HCC by anti-HCV response may not have been due to the ability of antiviral therapy to suppress HCC, but rather simply they may reflect the ability of such treatment to better identify patients at high-risk for HCC based on response to anti-HCV therapy.

It is not elucidated whether the results in our present analyses were simply due to the small number of

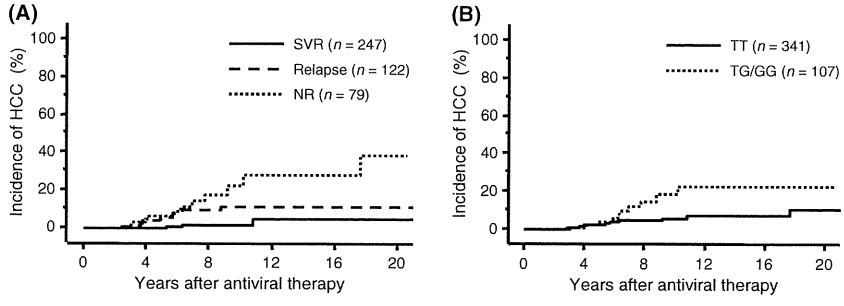

Fig. 1. Cumulative incidence of hepatocellular carcinoma (HCC) after antiviral therapy with interferon or peginterferon. (A) Incidence of HCC is significantly lower in patients with sustained virological response (SVR), those with relapse, and those with no response (NR) that includes partial response, viral breakthrough, or null-response, in that order. (B) Incidence of HCC is significantly lower in patients with TT genotype at rs8099917 near the *IL28B* gene, which is associated with the favourable response to antiviral therapy.

patients analysed or the incidence of HCC after antiviral therapy is similar regardless of response, when they are stratified by host and viral factors. In addition, our present analyses failed to examine the association between amino acid substitutions in the HCV core region and the incidence of HCC due to the small number of patients in whom the information of this substitution was available. Nonetheless, with the emergence of factors that can be independently associated with both the response to antiviral therapy and the development of HCC, the effect of response to antiviral therapy with IFN or PEG-IFN on the incidence of HCC will require re-examination taking *IL28B* polymorphisms and amino acid substitutions in the HCV core region into consideration.

Hidenori Toyoda and Takashi Kumada
Department of Gastroenterology, Ogaki Municipal Hospital, Ogaki, Japan

References

1. Imai Y, Kawata S, Tamura S, *et al.* Relation of interferon therapy and hepatocellular carcinoma in patients with chronic hepatitis C. *Ann Intern Med* 1998; **129**: 94–9.
2. Kasahara A, Hayashi N, Mochizuki K, *et al.* Risk factors for hepatocellular carcinoma and its incidence after interferon treatment in patients with chronic hepatitis C. *Hepatology* 1998; **27**: 1394–402.
3. Akuta N, Suzuki F, Sezaki H, *et al.* Association of amino acid substitution pattern in core protein of hepatitis C virus genotype1b high viral load and non-virological response to interferon-ribavirin combination therapy. *Intervirology* 2005; **48**: 372–80.
4. Ge D, Fellay J, Thompson AJ, *et al.* Genetic variation in IL28B predicts hepatitis C treatment-induced viral clearance. *Nature* 2009; **461**: 399–401.
5. Akuta N, Suzuki F, Kawamura Y, *et al.* Amino acid substitutions in the hepatitis C virus core region are the important predictor of hepatocarcinogenesis. *Hepatology* 2007; **46**: 1357–64.
6. Tillmann HL, Patel K, Muir AJ, *et al.* Beneficial *IL28B* genotype associated with lower frequency of hepatic steatosis in patients with chronic hepatitis C. *J Hepatol* 2011; **55**: 1195–200.
7. Abe H, Ochi H, Maekawa T, *et al.* Common variation of IL28 affects gamma-GTP levels and inflammation of the liver in chronically infected hepatitis C virus patients. *J Hepatol* 2010; **53**: 439–43.
8. Pekow JR, Bhan AK, Zheng H, Chung RT. Hepatic steatosis is associated with increased frequency of hepatocellular carcinoma in patients with hepatitis C-related cirrhosis. *Cancer* 2007; **109**: 2490–6.

Liver International (2012)

USING e-ANNOTATION TOOLS FOR ELECTRONIC PROOF CORRECTION

Required software to e-Annotate PDFs: Adobe Acrobat Professional or Adobe Reader (version 8.0 or above). (Note that this document uses screenshots from Adobe Reader X)
The latest version of Acrobat Reader can be downloaded for free at: http://get.adobe.com/reader/

Once you have Acrobat Reader open on your computer, click on the Comment tab at the right of the toolbar:

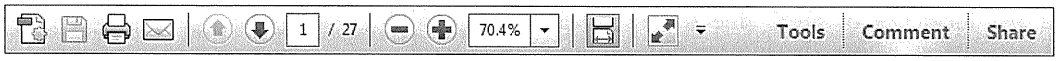

This will open up a panel down the right side of the document. The majority of tools you will use for annotating your proof will be in the Annotations section, pictured opposite. We've picked out some of these tools below:

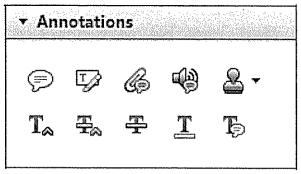

1. Replace (Ins) **Tool – for replacing text.**

Strikes a line through text and opens up a text box where replacement text can be entered.

How to use it

- Highlight a word or sentence.
- Click on the Replace (Ins) icon in the Annotations section.
- Type the replacement text into the blue box that appears.

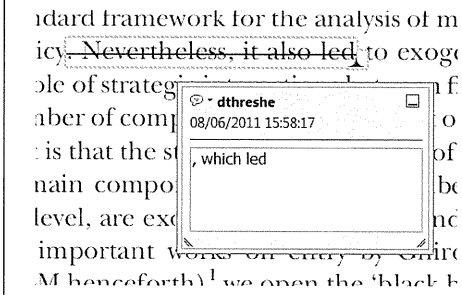

2. Strikethrough (Del) **Tool – for deleting text.**

Strikes a red line through text that is to be deleted.

How to use it

- Highlight a word or sentence.
- Click on the Strikethrough (Del) icon in the Annotations section.

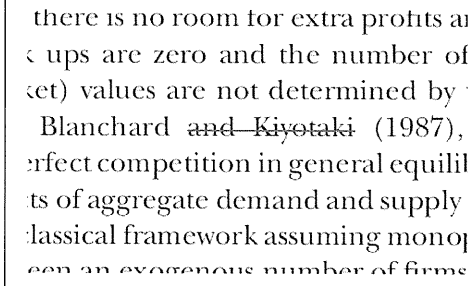

3. Add note to text **Tool – for highlighting a section to be changed to bold or italic.**

Highlights text in yellow and opens up a text box where comments can be entered.

How to use it

- Highlight the relevant section of text.
- Click on the Add note to text icon in the Annotations section.
- Type instruction on what should be changed regarding the text into the yellow box that appears.

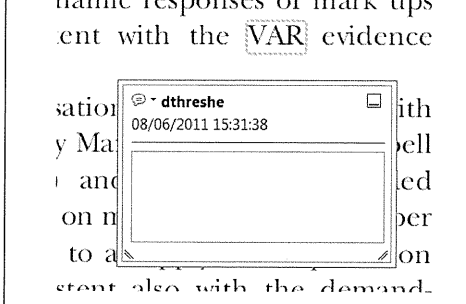

4. Add sticky note **Tool – for making notes at specific points in the text.**

Marks a point in the proof where a comment needs to be highlighted.

How to use it

- Click on the Add sticky note icon in the Annotations section.
- Click at the point in the proof where the comment should be inserted.
- Type the comment into the yellow box that appears.

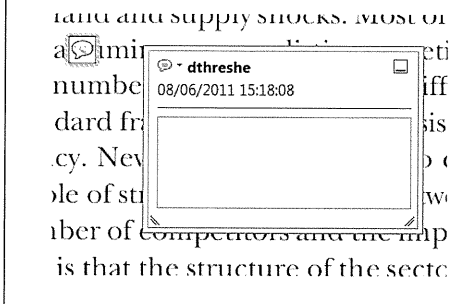

USING e-ANNOTATION TOOLS FOR ELECTRONIC PROOF CORRECTION

5. Attach File **Tool – for inserting large amounts of text or replacement figures.**

Inserts an icon linking to the attached file in the appropriate pace in the text.

How to use it

- Click on the Attach File icon in the Annotations section.
- Click on the proof to where you'd like the attached file to be linked.
- Select the file to be attached from your computer or network.
- Select the colour and type of icon that will appear in the proof. Click OK.

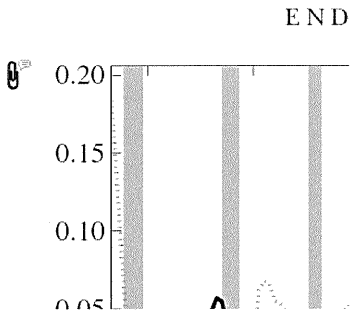

6. Add stamp **Tool – for approving a proof if no corrections are required.**

Inserts a selected stamp onto an appropriate place in the proof.

How to use it

- Click on the Add stamp icon in the Annotations section.
- Select the stamp you want to use. (The Approved stamp is usually available directly in the menu that appears).
- Click on the proof where you'd like the stamp to appear. (Where a proof is to be approved as it is, this would normally be on the first page).

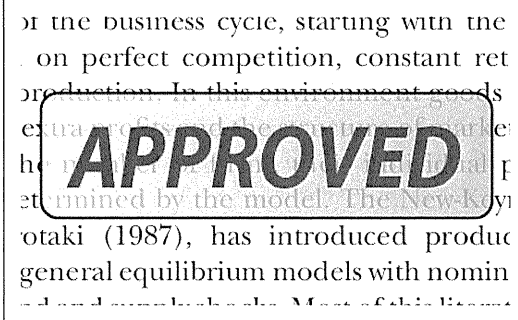

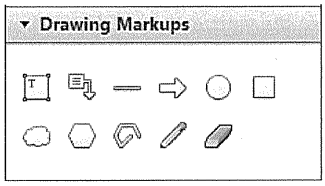

7. Drawing Markups **Tools – for drawing shapes, lines and freeform annotations on proofs and commenting on these marks.**

Allows shapes, lines and freeform annotations to be drawn on proofs and for comment to be made on these marks..

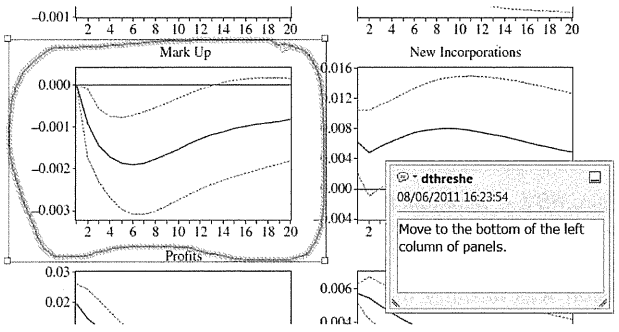

How to use it

- Click on one of the shapes in the Drawing Markups section.
- Click on the proof at the relevant point and draw the selected shape with the cursor.
- To add a comment to the drawn shape, move the cursor over the shape until an arrowhead appears.
- Double click on the shape and type any text in the red box that appears.

For further information on how to annotate proofs, click on the Help menu to reveal a list of further options:

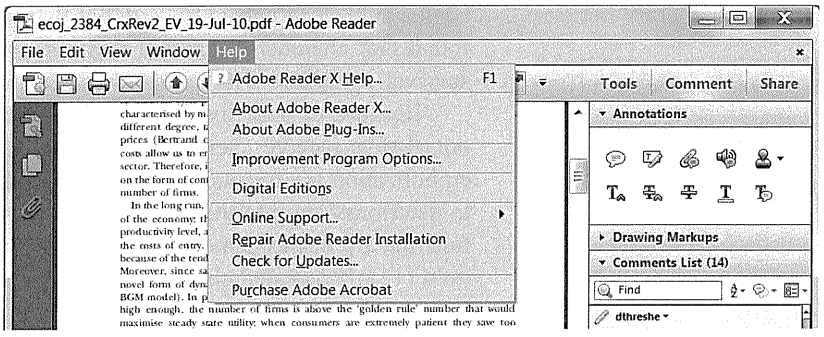

CLINICAL STUDY

Transarterial Chemoembolization for Hepatitis B Virus–Associated Hepatocellular Carcinoma: Improved Survival after Concomitant Treatment with Nucleoside Analogues

Hidenori Toyoda, MD, Takashi Kumada, MD, Toshifumi Tada, MD, Yasuhiro Sone, MD, and Masashi Fujimori, MD

ABSTRACT

Purpose: To determine whether nucleoside analogue therapy is associated with improved survival in patients with hepatitis B virus (HBV)–associated hepatocellular carcinoma (HCC) who are treated solely with transarterial chemoembolization.

Materials and Methods: A retrospective chart review of patients diagnosed with HBV-associated HCC was performed to identify patients treated solely with chemoembolization. Relevant demographic and clinical data were extracted and recorded. The influence of therapy with nucleoside analogues (lamivudine, adefovir dipivoxil, or entecavir) was determined by estimating the survival function using the Kaplan-Meier product-limit method.

Results: The inclusion criteria for chemoembolization were met by 81 patients (67 men and 14 women, mean age 60.6 years ± 9.2); 21 (25.9%) of these patients had been treated with nucleoside analogues. The number of chemoembolization treatments was significantly greater in the patients who were treated with nucleoside analogues (3.43 ± 2.32) than in the patients who did not receive nucleoside analogues (1.82 ± 0.95; $P = .0022$). The 1-year, 3-year, and 5-year survival rates were 89.5%, 66.8%, and 40.5% in the patients treated with nucleoside analogues and 72.6%, 27.5%, and 14.3% in the patients not treated with nucleoside analogues. The survival rate was significantly higher in the patients who received nucleoside analogues ($P = .0051$). Nucleoside analogue intake was an independent factor that was associated with increased survival ($P = .0063$).

Conclusions: Administration of nucleoside analogues was associated with longer survival in patients with HBV-associated HCC who were treated with transarterial chemoembolization.

ABBREVIATIONS

AFP = alpha-fetoprotein, HBV = hepatitis B virus, HCC = hepatocellular carcinoma

Transarterial embolization was initially used to treat hepatocellular carcinoma (HCC) by Doyon et al (1) in 1974, and chemoembolization with gelatin sponge particles and anticancer agents was subsequently developed in Japan to treat inoperable HCC (2). Despite the increase in the number of patients who undergo complete curative treatments such as hepatectomy or radiofrequency ablation (3), transarterial chemoembolization continues to have an important role, both as an initial treatment and as a therapeutic alternative for recurrent disease (4) because of the advanced nature of HCC at diagnosis and the high rate of recurrent disease (5). The benefits resulting from chemoembolization have long been a subject of debate (6–10), but two randomized trials found that chemoembolization was associated with higher survival compared with symptomatic treatment (4,11,12).

Because of poor liver function, patients with HCC do not always receive chemoembolization. Repeated chemoembolization treatments for HCC may cause liver function to deteriorate despite the fact that the deterioration of liver function by each chemoembolization treatment would be mild (13). If repeated chemoembolization treatments are to be used in cases of HCC recurrence, it is important to

From the Departments of Gastroenterology (H.T., T.K., T.T.) and Radiology (Y.S., M.F.), Ogaki Municipal Hospital, 4-86 Minaminokawa, Ogaki, Gifu, 503-8502, Japan. Received May 31, 2011; final revision received November 12, 2011; accepted November 14, 2011. Address correspondence to H.T.; E-mail: tkumada@he.mirai.ne.jp

None of the authors have identified a conflict of interest.

Tables E1 and E2 are available online at *www.jvir.org*.

J Vasc Interv Radiol 2012; xx:xxx

DOI: 10.1016/j.jvir.2011.11.012

prevent the worsening of liver function in the intervals between the treatments for longer survival (14).

Nucleoside analogues against hepatitis B virus (HBV) have been used since the late 1990s to suppress the replication of HBV and to normalize transaminase levels. Therapy with nucleoside analogues against HBV is known to arrest the progression of hepatic dysfunction in patients with chronic hepatitis B. More recent studies have shown that these drugs prevent the development of liver failure, even in the patients with advanced liver fibrosis (15–19). However, it is unknown whether this beneficial effect of antiviral therapy translates into longer survival for patients with concomitant HCC who undergo chemoembolization. We conducted a retrospective review of our experiences using chemoembolization to treat HCC in patients with chronic HBV infection.

MATERIALS AND METHODS

Patients

The complete study protocol was approved by the institutional review board of our hospital and was performed in compliance with the Helsinki Declaration. Between July 1997 and December 2010, 1,359 patients were diagnosed with primary HCC at our institution. Chronic HBV infection was confirmed in 260 of these patients, and 95 of these 260 patients were treated with chemoembolization. Of these 95 patients, 14 underwent treatments other than chemoembolization for recurrent HCC (4 underwent hepatectomy and 10 underwent radiofrequency ablation), and the remaining 81 patients had been treated with chemoembolization alone for recurrent HCC tumors. Our study retrospectively examined these 81 patients.

HCC was diagnosed based on clinical criteria (20) in all 81 patients. Specifically, the patients had a pertinent clinical background (chronic HBV infection) and typical imaging results. The tumor usually was detected by B-mode ultrasonography with typical HCC imaging features, including a hypoechoic tumor or a tumor with a mosaic pattern with a halo. HCC was diagnosed when a high-density mass was detected on arterial phase dynamic computed tomography (CT) images combined with a low-density mass on portal phase dynamic CT images obtained with a single or multidetector helical CT scanner. All of the patients with possible HCC tumors underwent angiography using a unified CT-angiography system (Interventional-CT; Toshiba, Tokyo, Japan) (21,22). CT during arterial portography and CT during hepatic arteriography were also performed to evaluate the progression of HCC (23).

The patients included 67 men (82.7%) and 14 women (17.3%), with a mean age of 60.6 years ± 9.2. The liver function at diagnosis was Child-Pugh class A in 49 patients (60.5%). At the time of diagnosis, 52 patients (64.2%) had multiple initial HCC tumors. HCC was accompanied by branch portal vein invasion in 18 patients (22.2%), but no patients had HCC invasion of the main portal vein trunks or the left or right main portal vein (**Table E1**).

Chemoembolization for Hepatocellular Carcinoma and Follow-Up after Treatment

The treatment decisions were based principally on the Japanese HCC treatment guidelines (24). The patients were initially assessed for their eligibility for hepatic resection and subsequent local ablative therapies, including percutaneous ethanol injection, percutaneous microwave thermocoagulation, and radiofrequency ablation. The patients who were not eligible for curative treatment with surgery, local ablative therapies, or a combination of both were offered chemoembolization. The patients with Child-Pugh class C (25) liver function and the patients with HCC invasion of the main portal vein trunks and left or right main portal vein were not offered chemoembolization. Chemoembolization was performed by injecting an emulsion of 50 mg of farmorubicin hydrochloride (Epirubicin; Adria Laboratories, Columbus, Ohio) or 100 mg of cisplatin (IA-Call; Nihon-Kayaku, Tokyo, Japan) dissolved in 5 mL of iopamidol (Iopamiron, 370 mg I/mL; Schering, Tokyo, Japan) and mixed with 5 mL of iodized oil (Lipiodol Ultra Fluid; Guerbet, Paris, France). This procedure was followed by an injection of gelatin sponge particles (Gelfoam; Upjohn, Kalamazoo, Michigan). The total dose of the injected emulsion was determined by the volume of the liver that would be embolized. An unenhanced CT scan was obtained to confirm complete deposition of the iodized oil in the lesion and to complete the treatment.

After the first chemoembolization treatment, the patients were followed for 2.39–118.6 months (median follow-up period 19.3 months) at our institution with ultrasonography and CT or magnetic resonance imaging performed every 3–6 months. Serum tumor markers (alpha-fetoprotein [AFP], *Lens culinaris* agglutinin-reactive AFP, and des-gamma-carboxy prothrombin) were monitored every 3 months. When elevated tumor markers were detected, an additional imaging examination (usually CT or magnetic resonance imaging) was performed to check for recurrence or progression of HCC. If recurrence or progression was confirmed, retreatment was considered. Retreatment decisions were also based on the Japanese HCC treatment guidelines. Repeat chemoembolization was considered as a retreatment option in patients who had HCC recurrence or progression.

Statistical Analyses

The intergroup differences were analyzed using χ^2 and Mann-Whitney U tests for categorical and quantitative data. The date of the initial HCC treatment (chemoembolization) was defined as time zero when calculating the patient survival rates. Surviving patients and patients who died from causes other than liver disease were censored in the survival analysis. Patients whose death was caused by HCC

Table 1. Clinical Characteristics of Patients Who Did and Did Not Receive Nucleoside Analogues

	Nucleoside Analogues (+) (n = 21)	Nucleoside Analogues (−) (n = 60)	*P* Value
Age (mean ± SD, y) (range)	60.3 ± 8.9 (46–81)	60.6 ± 9.3 (37–78)	.7957
Sex ratio (female/male)	3 (14.3%)/18 (85.7%)	11 (23.3%)/49 (76.7%)	.9274
Child-Pugh class (A/B)	14 (66.7%)/7 (33.3%)	35 (58.3%)/25 (41.7%)	.6773
Albumin (mean ± SD, g/dL)	3.65 ± 0.45	3.33 ± 0.79	.0372
Total bilirubin (mean ± SD, mg/dL)	1.22 ± 0.72	0.98 ± 0.85	.0844
15-minute retention rate of ICG (%)*	24.8 ± 12.3	19.6 ± 13.8	.0691
Prothrombin (%)	81.1 ± 19.5	79.7 ± 20.4	.8209
Platelet count (× 1,000/mL)	112 ± 52	143 ± 82	.1867
Tumor size (mean ± SD, cm) (range)	4.30 ± 2.94 (1.2–11.5)	4.40 ± 3.24 (1.0–16.0)	.8083
Tumor size (≤ 2 cm/> 2 cm and ≤ 5 cm/> 5 cm)	4 (19.0%)/11 (52.4%)/6 (28.6%)	17 (28.3%)/25 (41.7%)/18 (30.0%)	.6282
Tumor number (single/multiple)	9 (42.9%)/12 (57.1%)	20 (33.3%)/40 (66.7%)	.4333
Portal vein invasion (absent/present)	18 (85.7%)/3 (14.3%)	45 (75.0%)/15 (25.0%)	.4744
AFP (median, ng/mL) (range)	56.7 (0.9–3,132)	61.4 (0.8–1,304,200)	.7836
AFP (≥ 20 ng/mL/< 20 ng/mL)	13 (61.9%)/8 (38.1%)	35 (58.3%)/25 (41.7%)	.9746
AFP-L3 (median, %) (range)	0.5 (0–64.0)	6.2 (0–60.7)	.3658
AFP-L3 (≥ 10%/< 10%)	7 (33.3%)/14 (66.7%)	24 (40.0%)/36 (60.0%)	.7769
DCP (median, mAU/mL) (range)	94.0 (16–8,000)	62.0 (10–75,000)	.7997
DCP (≥ 40 mAU/mL/< 40 mAU/mL)	13 (61.9%)/8 (38.0%)	41 (68.3%)/19 (31.7%)	.7854

AFP = alpha-fetoprotein; AFP-L3 = *Lens culinaris* agglutinin-reactive AFP; DCP = des-gamma-carboxy prothrombin; ICG = indocyanine green test.
* ICG test was not performed in 14 patients.

or liver failure were not censored. The survival function was estimated using the Kaplan-Meier product-limit method (26), and the log-rank test (27) was used to analyze the differences in survival.

The Cox proportional hazards model (28) was used to perform a multivariate analysis of the factors related to survival. The following variables were analyzed: patient age and sex, Child-Pugh class (A/B), tumor size (≤ 2 cm/> 2 cm and ≤ 5 cm/> 5 cm), number of tumors (single/multiple), portal vein invasion (absent/present), and treatment with nucleoside analogues against HBV. The data analyses were performed using JMP statistical software, version 6.0 (Macintosh version; SAS Institute, Cary, North Carolina). All *P* values were derived from two-tailed tests; $P < .05$ was considered statistically significant.

RESULTS

Comparison of Patient Characteristics According to Nucleoside Analogue Intake

The anti-HBV nucleoside analogues had been administered to 21 of the 81 patients (25.9%). Among the 21 patients who had received nucleoside analogues, 7 patients had already been taking nucleoside analogues at the initial HCC diagnosis, and the remaining 14 patients started nucleoside analogues after diagnosis of HCC. Seven patients were taking 100 mg of lamivudine (Zefix; GlaxoSmithKline, Tokyo, Japan), eight patients were taking 0.5 mg of entecavir (Baraclude; Bristol-Myers Squibb, Tokyo, Japan), and six patients were taking lamivudine and 10 mg of adefovir dipivoxil (Hepsera, GlaxoSmithKline) because of the emergence of lamivudine-resistant HBV. **Table 1** compares the background characteristics of the patients who had and had not been treated with nucleoside analogues. There were no significant differences between these two groups in patient age and sex, liver function, and tumor progression, although the serum albumin levels were higher in the patients who received nucleoside analogues.

Influence of Nucleoside Analogue Treatment on Survival and Progression-Free Survival

Table 2 shows the number of chemoembolization treatments that were performed for initial and recurrent HCC with respect to the nucleoside analogue intake. Chemoembolization could not be performed more than four times in the patients who had not received nucleoside analogues; however, it was performed more than four times in one-third of patients who did receive them. The number of chemoembolization treatments was significantly higher in the patients who had received nucleoside analogues than in the patients who were not treated with nucleoside analogues ($P = .0022$). In the patients who underwent chemoembolization treatments repeatedly, the interval between two chemoembolization treatment sessions did not differ significantly between the patients who were and were not treated with nucleoside analogues (6.27 months ± 2.66 in patients without nucleoside analogues vs 6.71 months ± 2.71 in

Table 2. Number of Transarterial Chemoembolization Procedures Performed as a Function of Treatment with Nucleoside Analogues

No. Transarterial Chemoembolization Procedures	1	2	3	4	5	6	7	8
Nucleoside analogues (−) (n = 60)	28 (46.7%)	20 (33.3%)	7 (11.7%)	5 (8.3%)	0	0	0	0
Nucleoside analogues (+) (n = 21)	5 (23.8%)	4 (19.0%)	5 (23.8%)	0	3 (14.3%)	1 (4.8%)	1 (4.8%)	2 (9.5%)

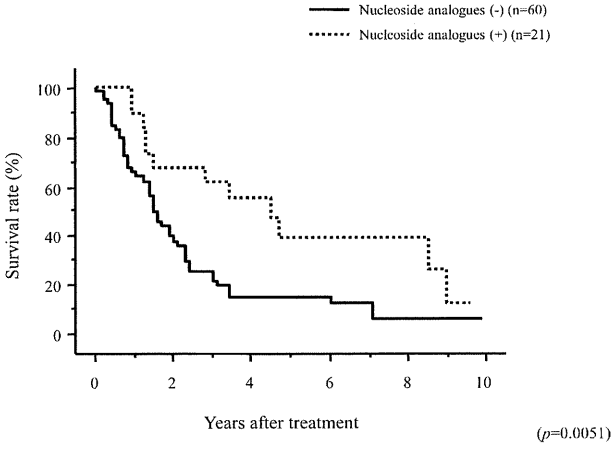

Figure 1. Plot of the Kaplan-Meier product-limit functions for survival after transarterial chemoembolization for initial HCC in the patients who did and did not receive nucleoside analogues.

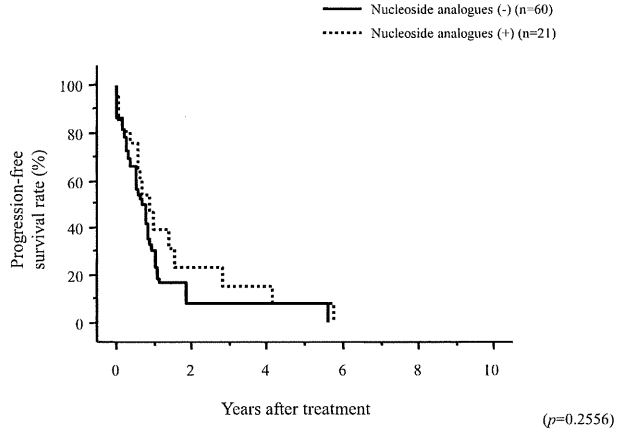

Figure 2. Plot of the Kaplan-Meier product-limit functions for progression-free survival after transarterial chemoembolization for initial HCC in the patients who did and did not receive nucleoside analogues.

patients with nucleoside analogues; $P = .3893$). The reasons for not offering further chemoembolization treatments to patients who did not receive nucleoside analogue therapy were emerging signs of liver failure (including ascites, jaundice, and hepatic coma) in 29 (48.3%) patients, progression to Child-Pugh C liver function in 18 (30.0%) patients, and progression of HCC (including extrahepatic metastases and invasion of the main portal vein trunks and left or right main portal vein) in 13 (21.7%) patients. The reasons for not offering further chemoembolization to the patients who did receive nucleoside analogue therapy were emerging signs of liver failure in 6 (28.6%) patients, progression to Child-Pugh C liver function in 4 (19.0%) patients, and HCC progression in 11 (52.4%) patients. Further chemoembolization was denied because of HCC progression more frequently in patients who were treated with nucleoside analogues ($P = .0174$).

Figure 1 shows the survival curves for the two patient groups. The 1-year, 3-year, and 5-year survival rates were 89.5%, 66.8%, and 40.5% in the patients treated with nucleoside analogues and 72.6%, 27.5%, and 14.3% in the patients who did not receive nucleoside analogues. The survival rate was significantly higher in the patients who were treated with nucleoside analogues ($P = .0051$). By contrast, there was no difference in the progression-free survival rates between the two groups ($P = .2556$) (**Fig 2**).

A multivariate analysis was performed to examine the factors that influenced survival after chemoembolization for the initial HCC (**Table 3**). Multiple tumors and portal vein invasion at the initial HCC diagnosis independently reduced the survival rate, and nucleoside analogue intake was an independent factor that increased the survival rate. When multivariate analysis included the number of chemoembolization treatments as an independent variable, the number of chemoembolization treatments was an independent factor associated with improved survival, and the statistical significance of nucleoside analogue intake disappeared (**Table E2**).

DISCUSSION

The results of the present study showed an association of nucleoside analogue therapy with longer survival in patients with HBV-associated HCC who were treated with chemoembolization for initial and recurrent disease. A multivariate analysis showed that nucleoside analogue intake was an independent factor that affected patient survival. However, the statistical significance of nucleoside analogue intake for improved survival disappeared when the multivariate analysis included the number of chemoembolization treatments as an independent variable, and the number of chemoembolization treatments was the factor that most affected survival. The patients who had received nucleoside analogues underwent a significantly greater number of chemoembolization treatments for HCC than the patients who were not treated with nucleoside analogues. Taken together, these results suggest that the association between nucleo-